PHILOSOPHICAL TRANSACTIONS OF THE ROYAL SOCIETY A MATHEMATICAL, PHYSICAL & ENGINEERING SCIENCES

High-Resolution n.m.r. in Solids with Strong Homonuclear Dipolar Broadening: Combined Multiple-Pulse Decoupling and Magic Angle Spinning [and Discussion]

B. C. Gerstein and K. J. Packer

Phil. Trans. R. Soc. Lond. A 1981 **299**, 521-546
doi: 10.1098/rsta.1981.0033

Phil. Trans. R. Soc. Lond. A **299**, 521–546 (1981)
Printed in Great Britain

High-resolution n.m.r. in solids with strong homonuclear dipolar broadening: combined multiple-pulse decoupling and magic angle spinning†

By B. C. Gerstein

Ames Laboratory, U.S. Department of Energy
and Department of Chemistry, Iowa State University, Ames, Iowa 50011, *U.S.A.*

The theory of homonuclear decoupling combined with magic angle spinning is developed in the average Hamiltonian formalism. A description of pulse sequences used to tune for pulse width, pulse phase difference, and to minimize phase transient impurities is given. Resolution of n.m.r. spectra of ^{1}H in crystalline, partly crystalline and amorphous solids under various pulse sequences with and without magic angle spinning are illustrated. Sources of residual broadening are discussed.

1. Introduction

Nuclear magnetic resonance may well be one of the most versatile tools available for probing the physical and chemical properties of matter, in situations where appropriate nuclei are available as probes. Longitudinal relaxation times in the laboratory frame may be used to infer motions at nuclear Larmor frequencies, as well as activation energies for such motion (Torrey 1954; Resing & Torrey 1963; Krüger 1969). Transverse relaxation times reflect average internuclear distances, and may be used to infer motion in some rigid solids (Hwang *et al.* 1978). Longitudinal relaxation times in the rotating frame are used to monitor motion at kilohertz frequencies (Slichter & Ailion 1964), and may be used to infer the degree of crystallinity of polymers (Conner 1970). Multiple quantum excitations (Vega *et al.* 1976) are used to monitor crystallinity in polymers (Vega 1980), motion, and shielding tensors of nuclei of spin greater than $\frac{1}{2}$. Applications include mechanisms of matter transport through biological membranes and elucidation of mechanisms of electronic conduction in superionic conductors (Polak *et al.* 1980). A particularly powerful method of studying diffusion in solutions (Stejskal & Tanner 1965), membranes (Silva-Crawford *et al.* 1980) and catalytically active solids (Taylor *et al.* 1980) involves analyses of the behaviour of the amplitudes of spin echoes under a variety of pulse experiments designed to 'refocus' specific interactions such as static field inhomogeneities or static dipolar interactions. There appear to be few problems in chemistry or physics not addressed in some manner by n.m.r.

There is clearly a wide diversity of parameters describing the response of an ensemble of nuclear spins to a resonant excitation. By far the most used, however, has been the shift of the frequency characterizing the isotropic chemical shift with change in chemical environment. The reasons for this popularity are clear. The isotropic chemical shifts of nuclei in molecules serve as both a qualitative and quantitative analysis for the molecular species present.

Because of the enormous bank of data on the ^{1}H and ^{13}C n.m.r. of model compounds, the

† This work is dedicated to the memory of Robert W. Vaughan, scientist, teacher and friend, who understood both science and people. His encouragement, help and goodwill made most of the work reported herein possible.

chemical shift spectra are subject to rapid identification. These shifts are relatively easily subject to measurement by technicians operating readily available commercial instruments.

The latter two statements have not applied until recently, and then with limitations (Ryan *et al.* 1980), to the use of n.m.r. to perform qualitative and quantitative analyses of molecules in the solid state. It is the purpose of this work to discuss some of the problems inherent in obtaining high-resolution n.m.r. of solids. The theory and experiment of techniques used to achieve currently achievable resolution in randomly orientated solids with strong homonuclear dipolar broadening will be described. Applications to attainment of parameters other than isotropic chemical shifts will be indicated.

2. Theory

(*a*) *Average Hamiltonian theory*

The usual detection of an n.m.r. signal rests upon the fact that an ensemble of nuclear spins, initially polarized along the z axis as determined by the static magnetic field, will develop a non-vanishing component of magnetic moment in the xy plane when disturbed from equilibrium. This component precesses about the z axis at the Larmor frequency, $|\omega_0| = |\gamma H_0|$ (42.5 MHz for protons at a field of 1 T (10^4 gauss)). The precession of this component in the xy plane induces a voltage in an inductor orientated with axis perpendicular to H_0, which is part of a resonant circuit tuned at ω_0. The observable, then, is a quantity proportional to $\langle I_y(t)\rangle$, the expectation value of the transverse component (here we assume phase detection along y in the rotating frame) of angular momentum. In terms of the density matrix representation of the time-dependent Schrödinger equation

$$\langle I_y(t)\rangle = \operatorname{tr} \rho(t)\, I_y, \tag{1}$$

where the density matrix operator, $\rho(t) = \psi(t)\,\psi^*(t)$, is given by the solution of the time-dependent Schrödinger equation (with $\hbar = 1$)

$$\mathrm{i}\frac{\partial \rho\ (t)}{\partial t} = [\mathscr{H}, \rho]. \tag{2}$$

A specification of $\rho(t)$, i.e. the r.h.s. of (2), will therefore specify the time decay of transverse magnetization observed in a pulse n.m.r. experiment. This time domain signal then bears a one–one relation to the frequency domain absorption signal via Fourier transformation (Anderson 1954):

$$I(\omega) \propto \operatorname{Re} \int_0^\infty \mathrm{e}^{-\mathrm{i}\omega t} I_y(t)\, \mathrm{d}t, \tag{3}$$

The Hamiltonian contains in general time-dependent and time-independent terms. $\mathscr{H}$ may be separated into terms controllable by the experimenter (the static and the radio-frequency fields), and those supplied internally by the system under study (dipolar fields, quadrupolar interactions, shielding, etc.). By appropriate demodulation, the experimentalist detects n.m.r. in the interaction frame of the Zeeman Hamiltonian, i.e. in the rotating frame. In this frame, the Zeeman interaction is absent, so it is appropriate to consider the Hamiltonian accessible to the experimenter as just $\mathscr{H}_{\mathrm{r.f.}}(t)$, the time-dependent (e.g. pulsed) radio-frequency interactions. For an ideal delta function pulse along x in the rotating frame, for example,

$$\mathscr{H}_{\mathrm{r.f.}} = -\gamma H_{1x} I_x \equiv -\omega_{1x} I_x, \tag{4}$$

and the condition that the magnetic moment be rotated by 90° is

$$-\int_0^t \mathscr{H}_{\text{r.f.}}(t')\,\mathrm{d}t' = \int_0^t \omega_{1x}\mathrm{d}t' = \int_0^{\frac{1}{2}\pi}\mathrm{d}\theta = \tfrac{1}{2}\pi. \tag{5}$$

In terms of rotation operators upon components of angular momenta, for example, a component of angular momentum along η operated on by a 'θ pulse' along ν will be transformed as

$$\mathrm{e}^{\mathrm{i}I_\nu\theta} I_\eta \mathrm{e}^{-\mathrm{i}I_\nu\theta} = I_\eta \cos(\theta\epsilon_{\nu\eta\lambda}) + I_\lambda \sin(\theta\epsilon_{\nu\eta\lambda}), \tag{6}$$

where ν, η, λ are some permutation of x, y, z. $\epsilon_{\nu\eta\lambda}$ is the Levi–Cévita symbol which is unity for ν, η, λ in cyclic order (e.g. z, x, y), -1 for anticyclic order (e.g. z, y, x), and 0 if $\nu = \eta$. So, for example,

$$\mathrm{e}^{\frac{1}{2}\mathrm{i}I_y\pi} I_z \mathrm{e}^{-\frac{1}{2}\mathrm{i}I_y\pi} = -I_x \tag{7}$$

is the operator equivalent of a 90° pulse along y rotating the z component of angular momentum to the negative x axis.

The Hamiltonians not accessible to the scientist (except by manipulation with $\mathscr{H}_{\text{r.f.}}$ (see below)) we term $\mathscr{H}_{\text{int}}$. Of primary importance to the present discussion are two internal Hamiltonians, the homonuclear dipolar Hamiltonian, which for the 1, 2 pair interaction is

$$\mathscr{H}_{\text{d}} = \alpha_{\text{d}}(3\cos^2\theta_{12} - 1)\,(\boldsymbol{I}_1 . \boldsymbol{I}_2 - 3I_{z_1}I_{z_2}), \tag{8}$$

where

$$\alpha_{\text{d}} = \tfrac{1}{4}\hbar\gamma^2/r_{12}^3\ \text{s}^{-1}, \tag{9}$$

and the anisotropic chemical shift interaction

$$\mathscr{H}_{\text{s}} = \alpha_{\text{s}}(3\cos^2\theta - 1)\,I_z, \tag{10}$$

where

$$\alpha_{\text{s}} = \omega_0\tfrac{1}{3}\{\sigma_{33} + \tfrac{1}{2}(\sigma_{11} + \sigma_{22})\}\ \text{s}^{-1}. \tag{11}$$

Here, θ_{12} specifies the direction between the internuclear vector r_{12} and the external magnetic field, and θ is the angle between the z axis of the shielding tensor, σ_{33}, and H_0.

In terms of $\mathscr{H}_{\text{r.f.}}$ and $\mathscr{H}_{\text{int}}$, (2) then becomes

$$\mathrm{i}\,\partial\rho/\partial t = [(\mathscr{H}_{\text{r.f.}} + \mathscr{H}_{\text{int}}), \rho]. \tag{12}$$

A transformation to the frame of $\mathscr{H}_{\text{r.f.}}$ is made formally as specified by the relation

$$\rho(t) = U_{\text{r.f.}}^{-1}\tilde{\rho}(t)\,U_{\text{r.f.}}. \tag{13}$$

$U_{\text{r.f.}}$ is determined by $\mathscr{H}_{\text{r.f.}}$ via the differential equation (with $\hbar = 1$)

$$\mathrm{i}\,\partial U_{\text{r.f.}}/\partial t = \mathscr{H}_{\text{r.f.}}\,U_{\text{r.f.}}. \tag{14}$$

In the frame of the r.f. the equation of motion of the density operator is

$$\mathrm{i}\,\partial\tilde{\rho}/\partial t = [\tilde{\mathscr{H}}_{\text{int}}, \tilde{\rho}]. \tag{15}$$

In this frame, $\mathscr{H}_{\text{int}}$ is controlled by $\mathscr{H}_{\text{r.f.}}$ via the relation

$$\tilde{\mathscr{H}}_{\text{int}}(t) = U_{\text{r.f.}}^{-1}\,\mathscr{H}_{\text{int}}\,U_{\text{r.f.}}. \tag{16}$$

Note that the effect of transforming to the frame of the r.f., i.e. (13), is to remove $\mathscr{H}_{\text{r.f.}}$ from the description of $\tilde{\rho}$ (equation (15)). In addition, $U_{\text{r.f.}}$ is a well known solution (Wilcox 1967) to (14); the operator that transforms from time 0 to time t is

$$U_{\text{r.f.}}(t, 0) = T\exp\left\{-\mathrm{i}\int_0^t \mathscr{H}_{\text{r.f.}}(t')\,\mathrm{d}t'\right\}, \tag{17}$$

where T is the Dyson time-ordering operator. It suffices here to say that if

$$\int_0^t \mathscr{H}_{\text{r.f.}}(t')\,\mathrm{d}t' = 0, \tag{18}$$

then $U_{\text{r.f.}}$ will be unity. Two obvious examples of cases where (17) becomes unity are: (i) $\mathscr{H}_{\text{r.f.}}$ is a π pulse at a given phase, followed by a π pulse with the same phase. This sequence corresponds to a rotation by 360°, which corresponds to no rotation at all (ignoring for the moment the subtleties of a spinor with $S = \frac{1}{2}$ transforming to itself under a 720° rotation (Stoll *et al.* 1977)), and (ii) an ideal $\frac{1}{2}\pi$ pulse in the rotating frame, followed by an equally ideal $\frac{1}{2}\pi$ pulse along the negative of that phase. Again the net transformation after the two pulses corresponds to leaving the spin system where it was before the pulse sequence. It is important to note at this point that the physics being implied is that of there being no interactions 'strongly' affecting ρ in the time over which $\mathscr{H}_{\text{r.f.}}(t')$ is integrated, i.e.

$$|\mathscr{H}_{\text{r.f.}}(t)| \gg |\mathscr{H}_{\text{int}}|. \tag{19}$$

Another way of saying this is that if dipolar fields are of order 0.5×10^{-4} T, then r.f. fields should be at least 5×10^{-3} T.† The time over which $\mathscr{H}_{\text{r.f.}}$ is applied must be short compared with T_2, i.e. short compared with the dipolar line width α_{d}. For protons with $\gamma = 4.25$ kHz/10^{-4} T, a value of a dipolar field of 5×10^{-4} T means a dipolar line width of roughly 20 kHz, so $T_2^* \approx 16$ μs.

The cycle time consideration may be formally expressed as the strong convergence condition for (23) (see below).

The process of removing an interaction from the description of ρ in a particular frame may be continued. The transformation

$$\tilde{\rho} = U_{\text{int}}^{-1}\tilde{\tilde{\rho}}U_{\text{int}}, \tag{20}$$

where U_{int} is determined by the Liouville equation

$$\mathrm{i}\,\partial U_{\text{int}}/\partial t = \tilde{\mathscr{H}}_{\text{int}}\,U_{\text{int}}, \tag{21}$$

leads to the result

$$\mathrm{i}\,\partial\rho/\partial t = [0, \tilde{\tilde{\rho}}] = 0, \tag{22}$$

i.e. $\tilde{\tilde{\rho}}$ appears static in this frame. At time $t = t_{\text{c}}$ the solution of (21) is given either by the Dyson expression, e.g. (17), or by the Magnus expansion (Wilcox 1967),

$$U_{\text{int}} = \exp\{-\mathrm{i}t_{\text{c}}[\bar{H}_{\text{int}}^{(0)} + \bar{H}_{\text{int}}^{(1)} + \ldots]\}, \tag{23}$$

where the zeroth-order term is given by

$$\bar{H}^{(0)} = \frac{1}{t_{\text{c}}}\int_0^{t_{\text{c}}} \tilde{\mathscr{H}}_{\text{int}}(t)\,\mathrm{d}t, \tag{24}$$

the first-order term by

$$\bar{H}_{\text{int}}^{(1)} = \frac{-\mathrm{i}}{2t_{\text{c}}}\int_0^{t_{\text{c}}}\mathrm{d}t\int_0^t \mathrm{d}t'\,[\tilde{\mathscr{H}}_{\text{int}}(t), \tilde{\mathscr{H}}_{\text{int}}(t')], \tag{25}$$

and higher terms by higher commutators. The density operator in the frame of detection at time t_{c} is given by

$$\rho(t_{\text{c}}) = U_{\text{int}}^{-1}U_{\text{r.f.}}^{-1}\tilde{\tilde{\rho}}U_{\text{r.f.}}U_{\text{int}}. \tag{26}$$

If $\tilde{\tilde{\rho}}$ is formally identified as $\rho(0)$, then (26) formally expresses a means of calculating the time development of ρ. If at time t_{c} both U_{int} and $U_{\text{r.f.}}$ become unity, then

$$\rho(t_{\text{c}}) = \rho(0), \tag{27}$$

† This would imply a 90° pulse width of 1.2 μs for protons.

and a measurement of an observable, as given by (1), at a time t_c, will yield the same result as at time $t = 0$; i.e. the measurement will not be effected by $\mathscr{H}_{\rm int}$ in particular. Specifically, if $\mathscr{H}_{\rm int}$ is the homonuclear dipolar interaction (equation (8)), then a measurement of the time decay of the transverse magnetization at time t_c will not appear to be damped by homonuclear dipolar interactions. If $\mathscr{H}_{\rm r.f.}$ is both cyclic,

$$T \exp\left[-\mathrm{i}\int_0^{t_c} \mathscr{H}_{\rm r.f.}(t)\,\mathrm{d}t\right] = 1, \tag{28}$$

and periodic,

$$\mathscr{H}_{\rm r.f.}(t+t_c) = \mathscr{H}_{\rm r.f.}(t), \tag{29}$$

then, via (16), $\tilde{\mathscr{H}}_{\rm int}$ will similarly be periodic, such that, for example, for the zero-order term at time $2t_c$,

$$\begin{aligned} U_{\rm int}(2t_c, 0) &= U_{\rm int}(2t_c, t_c)\, U_{\rm int}(t_c, 0) \\ &= \exp\{-\mathrm{i}\,\bar{H}^{(0)}_{\rm int} t_c\} \exp\{-\mathrm{i}\,\bar{H}^{(0)}_{\rm int} t_c\} \\ &= \exp\{-\mathrm{i}2t_c\,\bar{H}^{(0)}_{\rm int}\}, \end{aligned} \tag{30}$$

and at time nt_c for some multiple, n, of the cycle time,

$$U_{\rm int}(nt_c, 0) = U^n_{\rm int}(t_c, 0). \tag{31}$$

TABLE 1

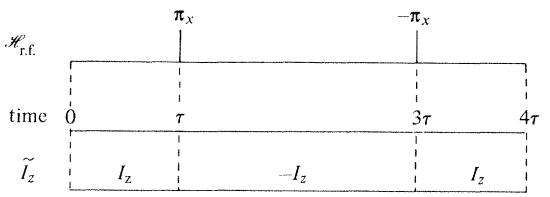

$$\int_0^{t_c} \mathscr{H}_{\rm r.f.}(t_z)\,\mathrm{d}t = \pi[I_x - I_x] = 0;\ U_{\rm r.f.}(4\tau, 0) = 2.\dagger$$

$$\frac{1}{t_c}\int_0^{t_c} \tilde{\mathscr{H}}_{\rm int}(t)\,\mathrm{d}t = \frac{1}{4\tau}[\tau I_z - 2\tau I_z + \tau I_z] = 0;\ U_{\rm int}(4\tau, 0) = 1.$$

† It will be instructive for the student to consider what will be the value of $\mathscr{H}_{\rm r.f.}$ at time 2τ.

The system therefore appears to be affected by some 'average' Hamiltonian, $\bar{H}^{(0)}_{\rm int}$, over the cycle time in question.

If $U_{\rm int}(t_c, 0)$ is unity, so will be $U_{\rm int}(nt_c, 0)$, and if $U_{\rm r.f.}$ is also unity at these times, both ρ and the expectation value of $I_y(t)$ will be unaffected by $\mathscr{H}_{\rm int}$ in the 'windows' at nt_c. A familiar example of this situation is the refocusing of a static field inhomogeneity, with operator $-\delta\omega I_z$, by a sequence of two π_x pulses, at echo (cycle) time 4τ, as indicated in table 1.

(*b*) *Refocusing of the homonuclear dipolar interaction in the absence of motion: dipolar echoes and multiple-pulse sequences; scaling*

(i) *Refocusing the dipolar interaction; dipolar echoes and multiple-pulse sequences*

The use of time-dependent experiments to average the spatial part of internal Hamiltonians was developed relatively early by Andrew *et al.* (1958) and by Lowe (1959). Subsequently, Waugh *et al.* (1968) and Mansfield (1971) used time-dependent radio-frequency pulses to

average the spin portion of the dipolar Hamiltonian, and to scale the shielding interaction (see below). Improved pulse sequences were subsequently developed by Mansfield (1973) and by Vaughan and coworkers (Rhim *et al.* 1973) and Burum & Rhim (1979). Basically all of the multiple-pulse homonuclear decoupling sequences are combinations of a two-pulse sequence that removes homonuclear dipolar interactions to zeroth order, i.e. $\bar{H}_{\mathrm{d}}^{(0)} = 0$. To understand how this 'dipolar echo' sequence works, consider the pulse sequence $[\tau, \mathrm{P}_x, \tau, \mathrm{P}_y, \tau]$, where P_i denotes a $(\frac{1}{2}\pi)_i$ pulse. The behaviour of I_z, and therefore the two spin Hamiltonian $I_{z_1} I_{z_2} \equiv Z$ under this sequence is indicated in table 2, along with the integral of the spin portion of $\tilde{\mathscr{H}}_{\mathrm{dip}}$ over the time $0 \leqslant t \leqslant 3\tau$. The following points are to be noted in the development of table 2. First, $\alpha_{\mathrm{d}}(\theta, r)$ is explicitly independent of time (the zero motion limit). Secondly, ideal delta function pulses have been assumed; therefore $\tilde{\mathscr{H}}_{\mathrm{int}}$ is undefined, and need not be considered during the pulse. Thirdly, the equation for $\tilde{\mathscr{H}}_{\mathrm{int}}$ is given by (16), and it must be kept in mind that if $U = \mathrm{P}_y \mathrm{P}_x$, then $U^{-1} = \mathrm{P}_x^{-1} \mathrm{P}_y^{-1}$.

TABLE 2

		P_x		P_y	
$\mathscr{H}_{\mathrm{r.f.}}$					
time	0	τ		2τ	3τ
$\tilde{I}_z$	I_z		$-I_y$		I_x
$\tilde{I}_{z_1}\tilde{I}_{z_2} \equiv \tilde{Z}$	Z		Y		X

$$\int_0^{3\tau} \tilde{\mathscr{H}}_{\mathrm{dip}}(t)\,\mathrm{d}t = \alpha_{\mathrm{d}} \int_0^{3\tau} (\tilde{\boldsymbol{I}}_1 . \tilde{\boldsymbol{I}}_2 - 3\tilde{I}_{z_1}\tilde{I}_{z_2})\,\mathrm{d}t = \alpha_{\mathrm{d}}\{3\tau \boldsymbol{I}_1 . \boldsymbol{I}_2 - 3\tau(X+Y+Z)\}$$
$$= 3\alpha_{\mathrm{d}}\tau[\boldsymbol{I}_1 . \boldsymbol{I}_2 - \boldsymbol{I}_1 . \boldsymbol{I}_2] = 0.$$

This example indicates that $\bar{H}_{\mathrm{d}}^{(0)}$, the zeroth-order homonuclear dipolar Hamiltonian vanishes under the $(\tau, \mathrm{P}_x, \tau, \mathrm{P}_y, \tau)$ solid echo sequence. Not treated are higher-order terms, such as $\bar{H}_{\mathrm{d}}^{(1)}$, $\bar{H}_{\mathrm{d-o}}^{(1)}$, $\bar{H}_{\mathrm{d-t}}^{(1)}$, $\bar{H}_{\mathrm{d}}^{(2)}$, $\bar{H}_{\mathrm{d}}^{(3)}$, where, for example, $\bar{H}_{\mathrm{d-o}}^{(1)}$ is the first-order term coupling the dipolar Hamiltonian and the resonance offset Hamiltonian, and t stands for phase transient impurity (see §3*a*). While the two-pulse sequence averages $\mathscr{H}_{\mathrm{d}}$ to zeroth order, higher-order dipolar terms are not removed. The use of symmetry in designing pulse sequences that cancel higher-order terms has been discussed by Mansfield *et al.* (1973). Recently, Burum & Rhim (1979) have developed 24-pulse and (essentially equivalent) 52-pulse sequences that cancel homonuclear dipolar terms to at least second order, but which still appear to have problems with cross terms involving dipolar and offset Hamiltonians.

My personal preference is to use the BR-24 for homonuclear decoupling in systems where the spectral width is sufficiently narrow that offsets of less than 1 kHz are necessary to prevent aliasing in a non-quadrature detection type experiment. Such a sample might be 4,4′-dimethylbenzophenone. On the other hand, there exist samples with a very wide range of spectral components, e.g. protons in coals (Gerstein *et al.* 1977), and protons in ZrXH_y (X = Br or Cl; $y = 0.5$ or 1.0) (Murphy & Gerstein 1979).

The pulse sequencing and timing for the MREV-8 and BR-24 pulse sequences are shown in figure 1. For a detailed discussion of average Hamiltonians under these sequences, and for

symmetry considerations used to design groups of pulses for averaging specific interactions and their cross terms, the reader is encouraged to consult Mansfield & Haeberlen (1973) and Burum & Rhim (1979).

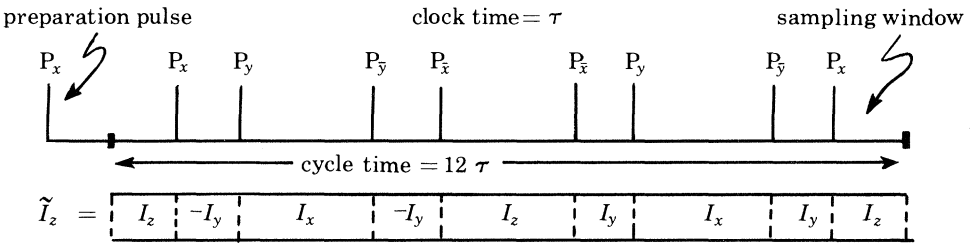

Mansfield–Rhim–Elleman–Vaughan 8-pulse with value of I_z in the frame of the r.f. indicated.

With the designations $1a = (XY)(\bar{Y})(\bar{X})$, $1b = (\bar{X}Y)(\bar{Y}X)$, $2a = (YX)(\bar{X}\bar{Y})$, $2b = (\bar{Y}X)(\bar{X}Y)$, MREV-8 may be written MREV-8 $= 1a1b$.

Similarly, BR-24 may be written BR-24 $= 1a1b2a(\bar{Y}X)2a2b(\bar{X}Y)$.

A preparation pulse along x would indicate that the appropriate phase detection would be along y.

FIGURE 1. Pulse sequences for MREV-8 and BR-24. Value of the offset operator, I_z, in the frame of the r.f. shown for the MREV-8.

Perhaps one of the greatest challenges to the ability of multiple pulse sequences to decouple homonuclear dipolar interactions is that of protons in linear, high-density, 95% crystalline polyethylene (h.d.l.p.), if one ignores solid H_2. As an example of the power of the MREV-8 and the BR-24 pulse sequences to narrow proton spectra in this material, the free precession response of protons in h.d.l.p. is compared with the first ten points of the decay under the BR-24 in figure 2*a*. Note that the free precession decay is over in about 15 μs, while the decay under the BR-24 clearly runs for more than 4000 μs. Figure 2*b* illustrates the powder pattern for protons in h.d.l.p. obtained from a Fourier transform of the decay under the MREV-8 at a cycle time of 21 μs. It is important to note that the BR-24 eliminates dipolar interactions to second order, while second-order dipolar interactions remain under the MREV-8. The second-

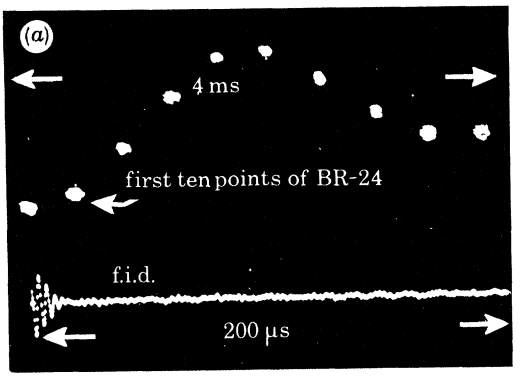

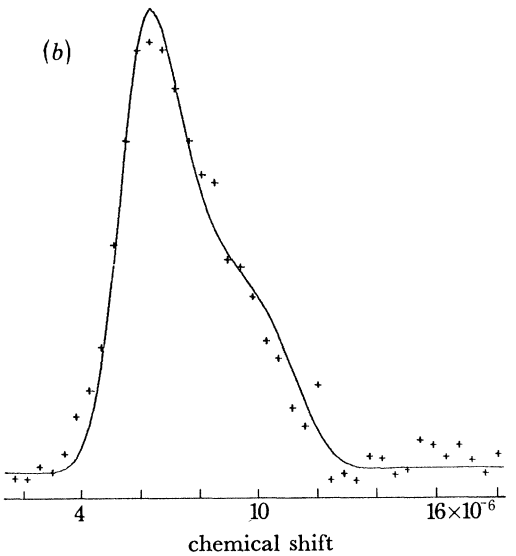

FIGURE 2. (*a*) Response of protons in high-density, linear polyethylene in the first ten windows of BR-24, compared with the response under a single-pulse excitation. (*b*) Fourier transform of the response of protons in this sample to MREV-8; cycle time, 21 μs; anisotropy, 4.72×10^{-6}.

order terms can be minimized by shortening the cycle time, which in turn shortens the observation window and therefore decreases the signal:noise ratio in the MREV-8 experiment. A very nice feature of the BR-24 experiment is that for sufficiently small resonance offsets (to minimize cross terms between offset and dipolar Hamiltonians), a 'clock time' of 3 μs will provide resolution equivalent to a clock time of 2.3 μs in the MREV-8 experiment on protons in ice (Burum & Rhim 1979; Ryan *et al.* 1977). Used here, the 'clock time' is the time interval between the two pulses in the dipolar echo experiment. Since the observation window is two clock time periods, the BR-24 provides an observation window of 6 μs, relative to 4.6 μs for the MREV-8. When one realizes that the observation window also includes the pulse width, and the combined ring-down of the probe–receiver chain, the total of which can be as long as 3.25 μs, even for probes with $Q = 20$, and with transmitters capable of a 0.8 μs 90° pulse

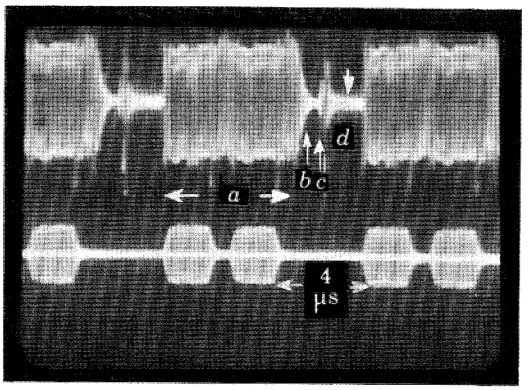

FIGURE 3. Comparison of signal detected at receiver output (top) and signal detected with antenna near probe (bottom). Receiver is one stage of an Avantek UTO 511 amplifier, followed by two stages of SML-D limiting amplifiers.

with such probes, it becomes apparent that the development of the BR-24 was an enormous boon to those wishing to do homonuclear decoupling with modest power. It is of course clear that the performance of such experiments is dependent upon the ability of the receiver chain to recover rapidly from the effects of an overload of the order of volts to sample microvolt signals, which may be as short as a few microseconds, in the sampling windows. The design of a receiver with rapid recovery characteristics has been published (Adduci *et al.* 1976). Characteristics of recovery of a similar receiver that I have used are shown in figure 3, which is an example of a pulse detected via an antenna near the r.f. coil of a probe used for homonuclear decoupling, compared with the response of the video portion of the amplifier chain detected at the output of the receiver (before the demodulation). Clearly seen in figure 3 is the power pulse washing through the receiver (region *a*), the dead period of the receiver during the ring-down of the pulse (region *b*), the recovery of the receiver (region *c*), and the period after recovery (region *d*). Details of crossed diodes shorting quarter-wavelengths to protect the receiver are available in Adduci *et al.* (1976).

A rough rule which is a valuable help in considerations involving times available for signal accumulation in observation windows of multiple-pulse experiments is that a probe with a given Q requires 21 time constants to ring down before undistorted signal can be detected. The time constant is roughly $Q/3f$. A probe with $Q = 20$ operating at 60 MHz would therefore be expected to 'completely' ring down in 2.3 μs. If the r.f. pulse width were 1 μs, the

minimum observation window for 0.5 μs signal accumulation would therefore be 3.8 μs, implying a clock time of 1.9 μs, or an 8-pulse cycle time of 22.8 μs (and a 24-pulse cycle time of 68.4 μs).

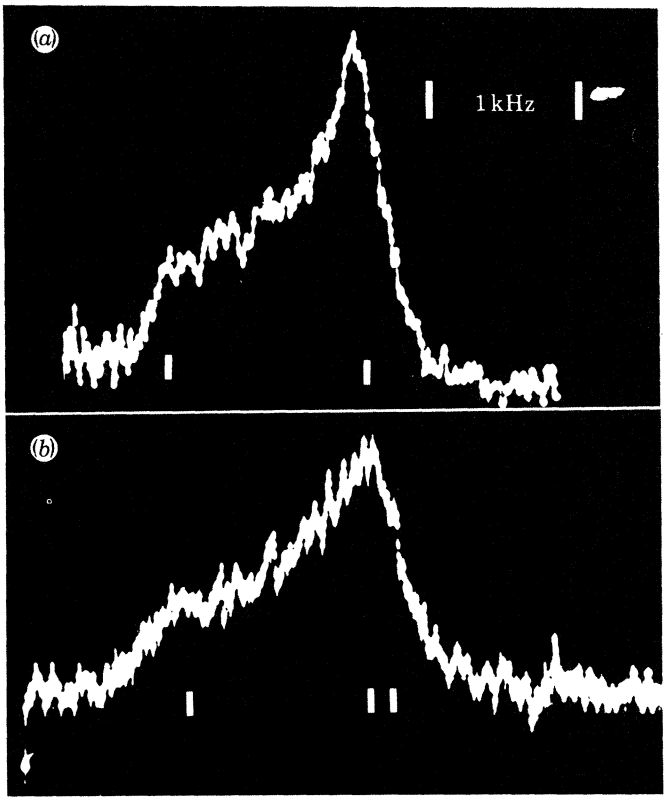

FIGURE 4. (*a*) Response of protons in squaric acid(s) to BR-24; Fourier-transformed decay. (*b*) Fourier-transformed decay of response of protons in the same system to BR-24 plus its mirror image (in which all odd homonuclear dipolar terms are eliminated).

It is interesting that while the BR-24 eliminates homonuclear dipolar interactions to second order, higher-order terms remain. A beautiful example of the manner in which symmetry can eliminate interactions is the use of the BR-24 followed by its mirror image to study the proton shielding tensor in squaric acid. The frequency spectrum obtained under the BR-24 is shown in the top plate of figure 4*a*. The spectrum under the 48-pulse sequence resulting from the BR-24 plus its mirror image, which eliminates all odd terms from the average dipolar Hamiltonian, is shown in figure 4*b*. The spectrum under the BR-24 could be axially symmetric. The spectrum under the 48-pulse sequence is clearly that of an asymmetric tensor.

In the above discussion, it has been mentioned that the use of the MREV-8 or the BR-24 depends on the spectral width of the sample under question when not using quadrature detection, because of the interaction between the offset and the dipolar terms. Rhim *et al.* (1976) have shown that the quadrature phase information is already present in the information available from the MREV-8 pulse spectrum, if sampling in appropriate windows and appropriate scaling of information from different windows is performed. Accomplishment of this task is then simply a matter of appropriate software development; in my opinion it would help performance of multiple-pulse experiments if it were a routine part of the experiment.

An already routine experimental procedure in my laboratory is the alternating of the preparation pulse in subsequent scans of a signal averaging routine between P_x and $P_{\bar{x}}$, with software sign changes of alternate scans in the signal accumulation process. This procedure eliminates baseline artefacts that are phase coherent from scan to scan, but are not phase coherent with the sign of the r.f. pulse (Stejskal & Schaefer 1975).

(ii) *Scaling*

In the free precession response to a single-pulse experiment, an ensemble of spins will oscillate about the offset field in the frame of detection. This is to say that the oscillation pattern in an f.i.d. reflects the fact that the component of spin along the transverse axis of detection is oscillating from positive to negative values with oscillation frequency given by the Larmor frequency corresponding to the effective field,

$$\omega = -\gamma H_{\text{offset}}, \tag{32}$$

reflecting the effective Hamiltonian corresponding to a field along z, H_{eff},

$$\mathscr{H}_{\text{eff}} = -\gamma I_z H_{\text{eff}} = -\boldsymbol{H}_{\text{eff}} . \boldsymbol{M}. \tag{33}$$

Under multiple-pulse sequences, the spin ensemble is moving (as observed in the cycle time observation windows) under some effective average Hamiltonian, which will be a sum of all average Hamiltonians present. In particular, for example, in the 'flip-flop' sequence used for tuning the phase of P_x against $P_{\bar{x}}$, the average Hamiltonian for an offset operator, with offset frequency $\Delta\omega$, is given by

$$\bar{H}_0^{(0)} = -\tfrac{1}{2}\Delta\omega(I_z - I_y) = -\gamma \boldsymbol{H}_{\text{eff}} . \boldsymbol{M}. \tag{34}$$

This interaction corresponds to a field pointing between z and $\bar{y}$. The magnitude of this field is $\sqrt{\frac{1}{2}}\Delta\omega/\gamma$. When compared with the magnitude of the field under a free precession decay, $\Delta\omega/\gamma$, it is seen that under the flip-flop experiment, the precession frequency is *scaled* by $(\sqrt{2})^{-1}$, i.e. frequencies under this multiple-pulse experiment are compressed (and timescales are expanded). The above discussion of scaling under the flip-flop sequence did not take into account the effect of finite pulse widths. This effect will be small if the time between pulses is large compared with the pulse width. An example of this scaling for the flip-flop experiment is shown in figure 5. In this figure, the first half of the decay is under the flip-flop sequence; the

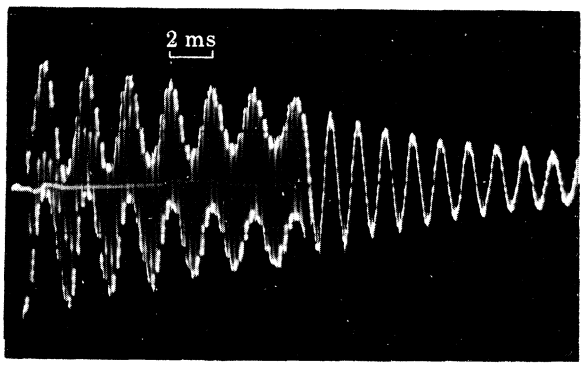

FIGURE 5. An example of scaling under the flip-flop cycle. The left portion of the decay is the flip-flop response of protons in water; the right half is free precession under an imposed offset identical to that imposed on the right portion of the signal. Note the difference in periods of both portions of decays.

PHILOSOPHICAL TRANSACTIONS OF THE ROYAL SOCIETY A MATHEMATICAL, PHYSICAL & ENGINEERING SCIENCES

sequence ends in the centre of the photograph, and the remainder of the decay is just a free precession under the imposed offset. The seriously interested student will want to compare the calculated result, above, with the scaling factor that can be measured on this photograph.

In exactly a similar manner, multiple-pulse homonuclear decoupling sequences have frequency responses under an offset that are scaled relative to the offset measured under a single-pulse excitation. Excluding the effects of finite pulse widths, the effective Hamiltonian of I_z under MREV-8 (i.e. an operator corresponding to offset, d.c. field inhomogeneities, etc.) is $\frac{1}{3}(I_x + I_z)$. This operator corresponds to a frequency scaling factor of $\frac{1}{3}\sqrt{2}$. This means that, for example, chemical shifts will be compressed by roughly a factor of two under the MREV-8. The scaling under the BR-24 is roughly $\frac{1}{9}2(3)^{\frac{1}{2}}$; chemical shifts are compressed by about 2.6. For every multiple-pulse experiment, the scaling factor will depend upon conditions of tuning and must be measured experimentally. This is accomplished by performing the multiple-pulse experiment on water and measuring the period of the offset beat under the multiple-pulse sequence relative to the period under a free precession with the same offset (see the discussion of the flip-flop sequence above). One way to do the measurement is to superpose a number of scans under the multiple-pulse experiment, each with offset differing by 1 kHz. The Fourier transform of this beat pattern will have peaks 1 kHz apart in real time, but less than 1 kHz apart in the digitized data, where the number of hertz per point are known from the dwell time and the number of points in the transform, i.e. (hertz per point in F.t.) = (dwell time × number of points in F.t.)$^{-1}$. For example, a dwell time of 0.2 μs per point, with a 2048-point transform, will yield 2.5 kHz per point in the frequency domain. When reporting shielding differences under multiple-pulse experiments, it must be kept in mind that frequencies are scaled, and must be corrected to convert observed differences into millionths.

(*c*) *The effect of motion upon homonuclear pulse decoupling*

In all of the above discussion, it has been assumed that the spatial part of the homonuclear dipolar Hamiltonian, $\alpha_d(r, \theta)$, is independent of time. If α_d becomes time-dependent because of a time-dependence in r_{ij} (vibration) or a time-dependence in θ_{ij} (libration), then these time-dependences must be included in the integrals of $\mathscr{H}_{int}$ over time. For purposes of illustration, suppose that α_d decays with some correlation time, τ:

$$\alpha_d(t) = \alpha_d(t = 0)\, e^{-t/\tau}.$$

Then in the dipolar echo sequence, the integral of $\mathscr{H}_{int}$ in the frame of the r.f. is, to zeroth order,

$$\begin{aligned} H_d^{(0)} &= \{\alpha_d(0)\}/t_c \int_0^{t_c} dt\, e^{-t/\tau}[\boldsymbol{I}_1 . \boldsymbol{I}_2 - 3I_{z_1} I_{z_2}] \\ &= \{\alpha_d(0)\}/t_c \{[e^{-t/\tau}\boldsymbol{I}_1 . \boldsymbol{I}_2]_0^{t_c} - 3[e^{-t/\tau}(X+Y+Z)]_0^t\}. \end{aligned} \tag{35}$$

If the correlation time, τ, is long compared with the cycle time, t_c, then the exponential in (35) may be expanded with the first term in the series being unity. Then the result shown in table 2 will obtain, i.e. to zeroth order, the dipolar Hamiltonian in the frame of the r.f., integrated over the dipolar echo sequence, will vanish. On the other hand, if the correlation time for motion is not long compared with t_c, the integral in (34) will not vanish, and the multiple-pulse experiment will be incapable of averaging the dipolar interaction. The latter result has been found in my laboratory for protons in yttrium hydride, $YH_{1.92}$ (unpublished).

PHILOSOPHICAL TRANSACTIONS OF THE ROYAL SOCIETY A MATHEMATICAL, PHYSICAL & ENGINEERING SCIENCES

(*d*) *Magic angle spinning and multiple-pulse decoupling*

Andrew *et al.* (1958) have shown that physical spinning of a sample about the angle that makes $(3\cos^2\theta - 1) \to 0$ (the 'magic angle') at angular speeds faster than the dipolar broadening, can average the dipolar broadening to zero. Physically realizable spinning speeds of 10 kHz have been achieved (Beams 1930; Andrew *et al.* 1969; Zilm *et al.* 1978), but these are not routinely attained. In addition, for systems containing protons or fluorine, it is not common to have dipolar broadening less than 10 kHz. One therefore asks if it is possible to couple the multiple-pulse experiment, in which r.f. pulses are used to remove dipolar broadening, with the magic angle spinning (m.a.s.) experiment, which removes interactions containing the term

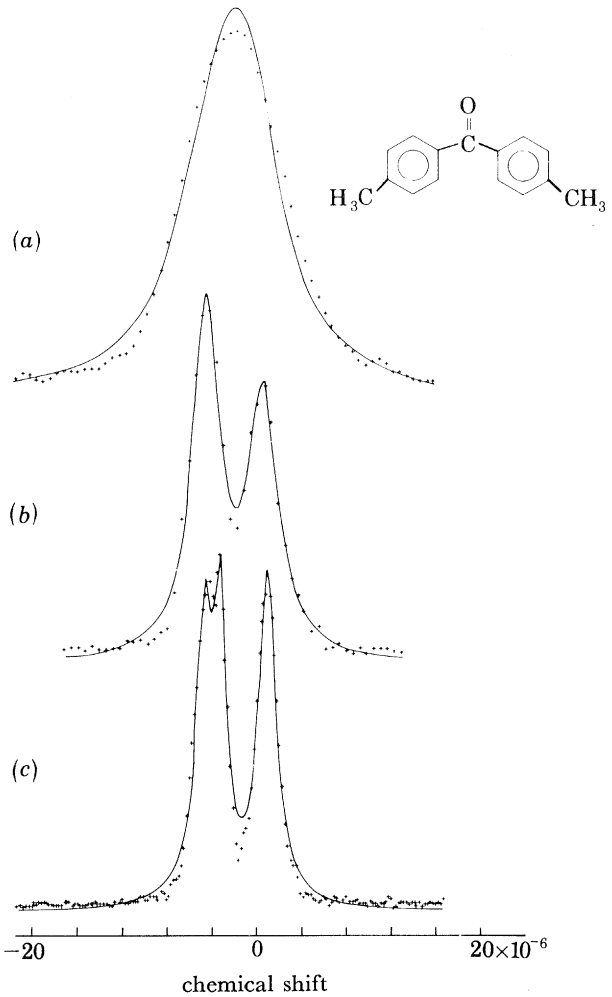

FIGURE 6. Frequency spectrum of protons in 4,4′-dimethylbenzoic acid under (*a*) MREV-8, (*b*) MREV-8 plus magic angle spinning and (*c*) BR-24 plus magic angle spinning.

$(3\cos^2\theta - 1)$. An example of the latter interaction is chemical shielding anisotropy. The necessity of removing both shielding anisotropies and dipolar broadening to achieve high-resolution spectra of strongly dipolar broadened powdered solids becomes apparent when it is realized that shielding anisotropies of, for example, protons in solids, *for a given chemical species*

of hydrogen, can be as large as ten times the total isotropic shift range (Murphy & Gerstein 1979). The powder spectrum of protons in a given molecule, e.g. 4,4′-dimethylbenzophenone, will therefore be a hopelessly jumbled overlap of different tensor powder patterns, with not much chemical information available, even if all dipolar broadening is removed.

The possibility of combining m.a.s. and homonuclear decoupling was discussed by Haeberlen & Waugh (1968), and first achieved 9 years later (Gerstein *et al.* 1977; Taylor *et al.* 1979; Ryan *et al.* 1980). The problem of immediate concern in such an experiment is that, as in the discussion in the preceding section on the effect of motion on the ability of the multiple-pulse sequence to narrow, rotation automatically introduces motion. The details of the mathematical description of the combined experiment are messy, and in my opinion lend little to an enhanced understanding of why the experiment works. Either Haeberlen & Waugh (1968) or Taylor *et al.* (1979) may be consulted for these details. The important physics contained in those treatments is the result that if the cycle time for physical rotation is very long compared with the cycle time for multiple-pulse decoupling, the experiment essentially reverts back to the static case as far as the pulse homonuclear decoupling is concerned. Uncharacteristically of Nature's usual behaviour, it has been quite kind in this instance. Since dipolar line widths in hydrogen- and fluorine-containing solids are generally 20 kHz or more, it is necessary to use multiple-pulse cycle times of about 30 μs for efficient decoupling. Proton anisotropies are usually less than 2 kHz, so the rotation period needed for efficient averaging of shielding anisotropies can be 500 μs. The ratio of the multiple-pulse cycle time to the physical rotation cycle time is therefore about 0.1. This ratio has experimentally been found to be sufficient for removing the effect of physical rotation on the multiple-pulse decoupling (Ryan *et al.* 1980). I have not been successful in finding a naturally occurring sample in which proton dipolar broadening is of order of easily attainable rotational frequencies, to investigate the details of the interaction between the dipolar decoupling and m.a.s. experiments. One could, of course, produce such a sample by appropriate doping of deuterium.

A good example of the progression of resolution of proton spectra in the powdered crystalline material 4,4′-dimethylbenzophenone as one proceeds from (*a*) multiple-pulse decoupling by MREV-8, but no m.a.s. to (*b*) multiple-pulse decoupling by MREV-8 with m.a.s. at 2.5 kHz to (*c*) multiple-pulse decoupling with BR-24 and m.a.s. at 2.5 kHz, is shown in figure 6. Further examples of resolution as a function of cycle time and offset on samples with varying crystallinity will be shown in §3.

(*e*) *Evaluating contributions to line widths*

For spin $\frac{1}{2}$ nuclei in solids, the main contributions to the n.m.r. line widths under a single-pulse experiment are dipolar broadening and shielding anisotropy, provided the lifetime broadening associated with, for example, the presence of paramagnetic centres is negligible. One usually evaluates lifetime broadening in liquids with experiments which refocus the I_z operator, e.g. with spin–echo experiments. When dipolar broadening is attenuated for spin $\frac{1}{2}$ species in solids by multi-pulse decoupling, residual contributions to the line width include: (*a*) higher-order dipolar terms, $\bar{H}_{\mathrm{d}}^{(i)}$, $i = 1, 2, \ldots$, which become less important as the cycle time is decreased; (*b*) higher-order cross terms between the dipolar interaction and interactions such as the offset Hamiltonian, e.g. $\bar{H}_{\mathrm{d-o}}^{(1)}$, the first-order term between the dipolar and offset Hamiltonians; (*c*) lifetime broadening under the multiple-pulse experiment; and (*d*) dispersion in local d.c. fields seen by individual nuclei, e.g. chemical shift dispersion associated with a

non-crystalline sample, or dispersion of demagnetization fields associated with irregular boundary conditions on small crystallites. A number of experiments have been developed to evaluate these individual contributions to line widths. These results of the coupling of the theory and experiment of transient techniques in magnetic resonance represent perhaps one of the most beautiful examples of selectively probing matter with quite delicate fingers, and are an example of the enormous power lent to magnetic resonance by the use of time as an added variable. All of these experiments depend upon the fact that a particular spin operator can be selectively averaged by multiple-pulse experiments. For example, in §2*a* we saw how the simple Hahn spin–echo experiment could be used to average the field gradient operator, which is proportional to I_z. In fact, this experiment will average any operator proportional to I_z in the observation window (i.e. at the peak of the echo), so both chemical shifts and field dispersion due to susceptibility effects will similarly be averaged by this spin–echo sequence. The immediate application to measurement of T_2 under a multiple-pulse experiment is to couple the multiple-pulse experiment with a 180° refocusing pulse along the appropriate direction in the rotating frame (Dybowski & Pembleton 1979). An alternative is to couple the multiple-pulse sequence with an operator perpendicular to the interactions that one wishes to average (Dybowski & Vaughan 1975). Where the second operator is sufficiently large compared with the first, the effect is to 'second average' (Haeberlen *et al.* 1971) the first operator. In both of the above experiments, the operator that is averaged is I_z, so from all residual broadening terms those proportional to I_z are selectively removed. The difference in decay times under the experiment with and without selective removal of I_z can then be used to infer broadening associated with terms proportional to I_z.

For the Dybowski–Pembleton (1979) dipolar narrowed Carr–Purcell (DNCP) experiment, the physics is quite easy to understand. The experiment is essentially the Carr–Purcell spin–echo sequence, with a multiple-pulse dipolar averaging sequence being sandwiched in the windows between the 180° refocusing pulses to remove the effect of dipolar dephasing. If the MREV-8 sequence, for example, is used to remove dipolar broadening, then in the scheme of shorthand notation used by Rhim (1979) to denote pulse sequences, as indicated in figure 1, the DNCP sequence would be denoted by $1a1b\ (180^\circ_y)\ 1a1b$. This sequence would be repeated n times (e.g. n might be 1024) after a preparation pulse P_x. The magnetization would be sampled in the 2τ window after the second $1b$ dipolar echo pair. These 1024 samples would then provide a decay, the time constant of which would be characterized by higher-order dipolar interactions and cross terms, but not by chemical shifts, susceptibility dispersion, etc. It should be noted here that a general theory of relaxation of spins under periodic irradiation has been developed by Vega & Vaughan (1978). Note that the 180° refocusing pulse is along the y phase, and in the window between the two multiple-pulse narrowing sequences. This phasing is critical, because with an x preparation pulse, the magnetization will lie along y after the multiple-pulse sequence, and must be minimally disturbed before the application of the next multiple-pulse narrowing sequence. A 180° pulse along x will indeed refocus I_z but will leave the spins in an inappropriate direction for detection along y in the next sampling window.

For the technique of second averaging, two sequences have been used as variations of the MREV-8. These have been denoted as $\mathrm{P}_x - \mathrm{M}_y$ (Lau *et al.* 1977; Dybowski & Vaughan 1975) and $-\mathrm{M}_x$ (Lau *et al.* 1977). In both of these experiments, a deliberate phase error $\varphi_{x,\bar{x}}$ is introduced along x or $\bar{x}$, i.e. the phase of the nominal x pulse has a

deliberately introduced y component. The zero-order average Hamiltonian introduced under the MREV-8 is

$$\bar{H}_{\mathrm{p}}^{(0)} = 2(\varphi_{\bar{x}} - \varphi_x)\, I_y/t_{\mathrm{c}}. \tag{36}$$

In the $\mathrm{P}_x - \mathrm{M}_y$ version, an x prepulse is applied, with observation of the magnetization along y in the rotating frame. Under MREV-8, the operator I_z becomes proportional to $\frac{1}{3}(I_x + I_z)$ (Rhim *et al.* 1974). This fact is immediately obvious from the entries of figure 1 under the MREV-8 sequence, for the value of $\tilde{I}_z$. The operator I_y (equation (36)) is perpendicular to the operator $(I_x + I_z)$. The magnetization of the system will precess about an effective field associated with the net average Hamiltonian $a(I_x + I_z) + bI_y$. If b is sufficiently large compared with a, the contribution of the term in $(I_x + I_z)$ will become negligible, and this operator will be 'second averaged' by the term in I_y. In a similar manner, the second-order dipolar Hamiltonian under the MREV-8 will become second averaged by a sufficiently large I_y component. Therefore, in the $\mathrm{P}_x - \mathrm{M}_y$ experiment, both chemical shifts and shielding anisotropies, as well as dipolar terms to second order, are removed. Residual broadening contains higher-order dipolar terms, cross terms between dipolar and other interactions, and lifetime broadening under the MREV-8. For the $-\mathrm{M}_x$ version of the MREV-8, no x prepulse is applied and observation of the magnetization is along x in the rotating frame. Under this sequence, higher-order dipolar terms remain, but terms in shielding and field inhomogeneity disappear. It is important to realize that both of these experiments depend upon being able to make the error Hamiltonian large compared with the terms that one wishes to second average. It may not always be possible to do this, e.g. when shielding anisotropies are as large as 100×10^{-6} (Murphy & Gerstein 1979).

3. Experiment

(*a*) *Tuning sequences: pulse width, phase and phase transients*

It must be clear by now that multiple-pulse narrowing experiments involve application of a series of pulses of a given pulse width and phase, followed by an observation of the magnetization in response to these pulses in an observation window between sequences. This observation is repeated many (e.g. 1024 or 2048) times. Small errors in pulse widths, pulse phase, and pulse transient phase glitch (but see Mansfield & Haeberlen 1973) will therefore accumulate quickly and kill the experiment unless care is taken in tuning and sequences are designed to minimize these effects. In the present discussion, a description of the tuning procedure used in my laboratory will be given. There are certainly other procedures, and the number must only be limited by the experimenter's imagination. The following sequence of tuning steps seems to work well with us.

1. All phases are tuned for pulse width adjustment. The sequence used is a string of pulses of a given phase, with phase detection orthogonal to the pulse in question and 100–200 μs between pulses. The sample used for tuning is protons in a paramagnetically doped spherical sample of water. The response of such a sequence over a 1 ms period and over a 4 ms period is indicated in figure 7*a*, for well tuned 90° pulses. The '+, 0, −, 0, +, ...' pattern clearly indicated at the top of figure 7*a* is exactly what one would expect from a series of 90°_i pulses with phase detection at $i + 90°$.

2. With the x channel being used as the reference phase, the phase of $\bar{x}$ is tuned with respect to x. The physics of changing the phase of $\bar{x}$ can be accomplished with constant impedance trombone-type line stretchers, or with a lumped circuit constant impedance phase shifter such

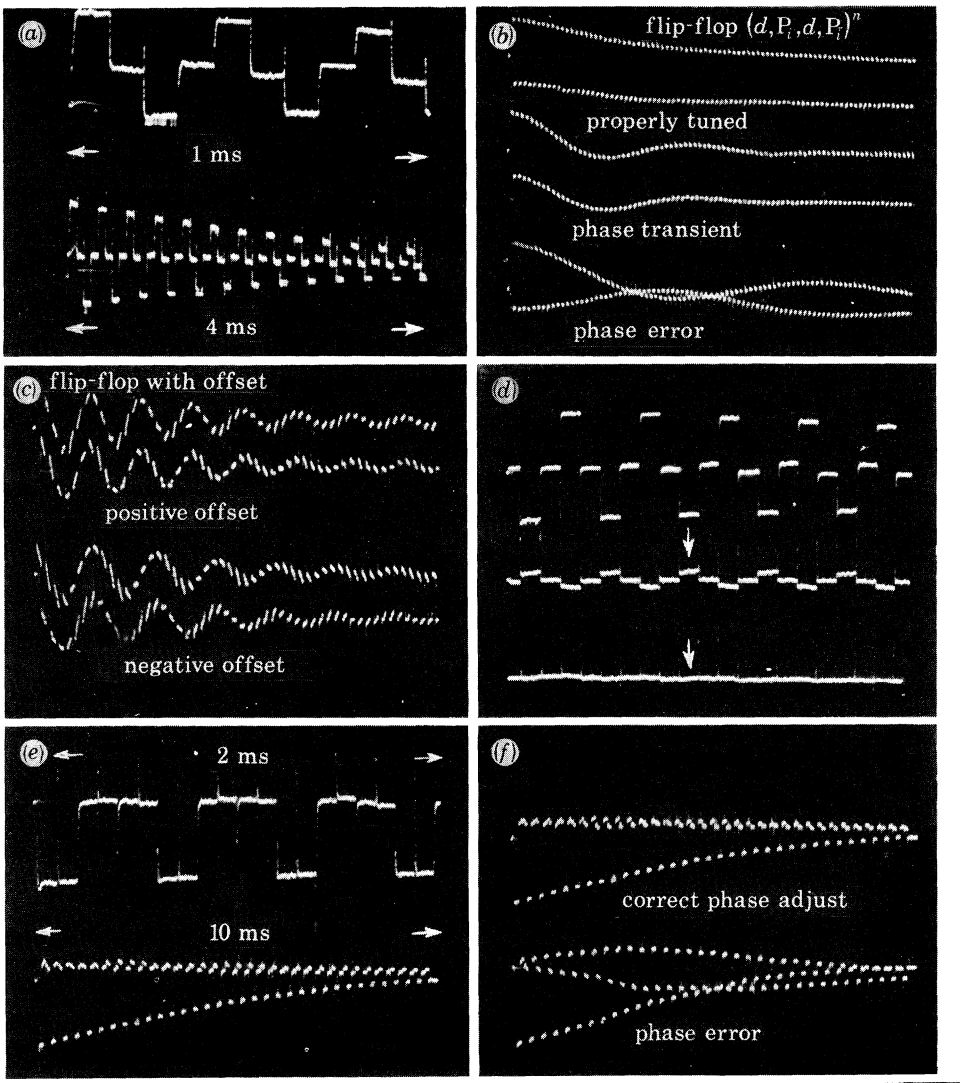

FIGURE 7. Response of protons in doped water to tuning sequences used to adjust (*a*) pulse widths, $(P_i)^n$, (*b*) phase of x against $\bar{x}$, (*c*) phase transients, (*d*) phase orthogonality, (*e*) phase of x against y, $(d, P_x, d, P_y)^n$, and (*f*) phase of y against x.

as a Merrimac PSS 2-30. The tuning sequence used for phase adjustment is the 'flip-flop' sequence, which is $(100\ \mu s, 90^\circ_x, 100\ \mu s, 90^\circ_{\bar{x}})^n$, where n is usually about 100. A properly tuned flip-flop sequence has a response shown at the top of figure 7*b*. Again, the '+, 0, +, ...' decay is exactly what one would expect (with even less reflexion than with the pulse width tuning sequence) for the response to the flip-flop. The initial droop at the beginning of the response has to do with d.c. drift in the receiver chain, and is a common feature of the response of multi-pulse spectrometers with which I am familiar. The average Hamiltonian for a phase transient impurity under this sequence (Rhim *et al.* 1974) is proportional to the operator $(I_z - I_y)$. In addition, the average Hamiltonian for an offset operator is given by

$$\bar{H}_0^{(0)} = \tfrac{1}{2}(I_z - I_y)\ \Delta\omega, \tag{37}$$

which has the same operator dependence as does the phase transient impurity, but which *changes sign* with the offset, $\Delta\omega$, *which the* operator for the transient *does not*. Therefore, if a

transient impurity is present, and one observes the flip-flop cycle in the presence of an imposed offset, $\pm\Delta\omega$, the apparent offset, should change depending upon whether the imposed offset is plus or minus. The flip-flop in the presence of a phase transient impurity is shown as the centre scan in figure 7*b*. Under single pulse excitation, the proton signal is on resonance. Under the flip-flop, there is an apparent offset. The flip-flop with positive and with negative offset in the presence of a phase transient impurity is shown in figure 7*c*. Note that the apparent offset is different in the two cases, indicating the presence of a phase glitch that is not cancelled under this sequence. Removal of this phase glitch is accomplished by proper matching of the impedances of the probe and transmitter. Such matching can be accomplished by using the fact that a pi circuit is the equivalent of a quarter-wavelength coaxial cable, with characteristic $Z_{\text{in}}Z_{\text{out}} = Z^2_{\text{cable}}$ (Murphy & Gerstein 1978). In my laboratory, insertion of a pi circuit between transmitter and probe, with components properly adjusted to match transmitter and probe, both with known impedance–frequency characteristics, is used to tune out the phase transients. Ultimately, the response of a water sample to the multiple-pulse sequence under question is used for fine tuning of transients. Tuning capacitors at the output of the transmitter, of course, will change the power seen by the probe, so the tuning must be recursive, in the sense that after this adjustment, the pulse widths must again by adjusted.

3. The phases of y and $\bar{y}$ are now tuned relative to the phase of x. An important part of this procedure is the exact adjustment of the phase shifter in the demodulation portion of the circuit, such that the phase being detected is exactly orthogonal to the phase seen when observing the response to an x pulse. With a string of $90^\circ_{\bar{x}}$ pulses exciting the system, the observation phase is tuned (figure 7*d*) until minimum signal is observed. At this point, observation is along x in the rotating frame. Then the sequence (100 μs, P_x, 100 μs, $\mathrm{P}_y)^n$, with n about 100, is used. The response of protons in water to such a sequence is a (0, 0, 0, 0, –, –, ...) decay shown in figure 7*e*. At the top of figure 7*e* is a 1 ms scan of the response, to indicate the details. At the bottom of figure 7*e* is shown 4 ms of the response, to indicate the general pattern for properly phased y with respect to x. In figure 7*f* is indicated the response of protons in water to a properly phased (top) and improperly phased (bottom) sequence $(d, \mathrm{P}_x, d, \mathrm{P}_y)^n$.

It must be kept in mind that in all of the tuning just described, it is assumed that there is not much adjustment to be done, either in phasing, tuning of transients, or pulse widths. Major adjustments are made when the instrument is first set up (with the exception of pulse widths, which can be controlled in an analogue fashion, or in a digital fashion on our instrument). There are many possibilities for construction of pulse programmers for the digital control of pulse channels. The unit in use in my laboratory is described in a recent publication (Adduci & Gerstein 1979), and has been found to be satisfactory for a wide but finite range of experiments.

(*b*) *Experimental results*

(i) *Simple crystalline solids and polymers*

The spectrum of ^{1}H in 4,4′-dimethylbenzophenone under the combination use of the BR-24 for homonuclear decoupling, and magic angle spinning has been shown in figure 6. In figures 8 and 9 are shown the combined rotation and multiple-pulse spectra (Cramps) of protons in aspirin, and in 2,6-dimethylbenzoic acid with the use of BR-24 for homonuclear decoupling. Ring, methyl and hydroxyl protons are clearly separated, and in the 2,6-DMB spectrum one can see a hint of splitting of the ring protons. 4,4′-Dimethylbenzophenone, aspirin, and 2,6-

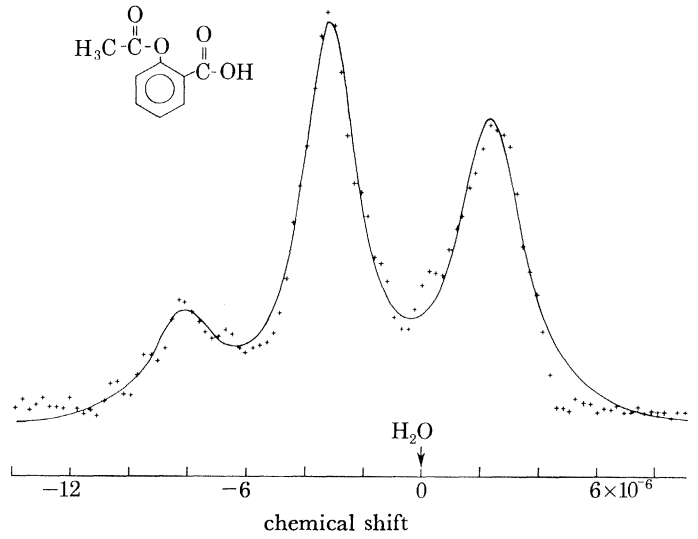

FIGURE 8. N.m.r. spectrum of protons in aspirin under combined rotation and multiple-pulse spectroscopy (CRAMPS). BR-24 used for homonuclear decoupling.

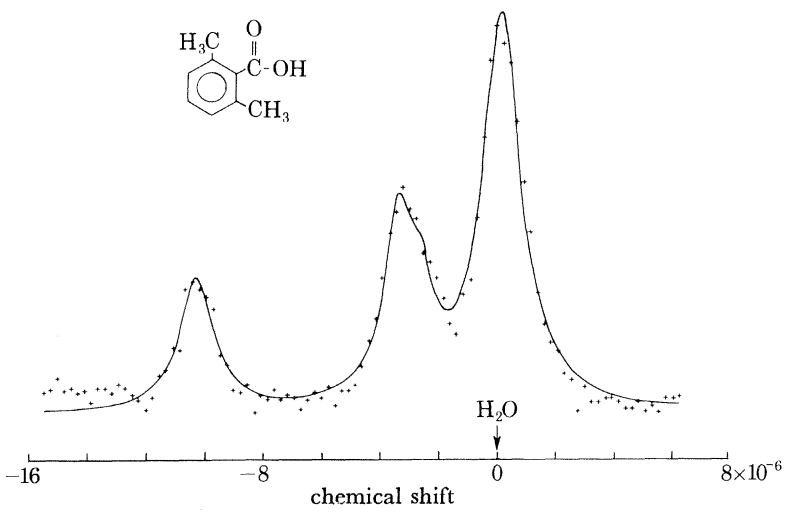

FIGURE 9. CRAMPS spectrum of ^1H in 2,6-dimethylbenzoic acid.

DMB are considered to be examples of well defined crystalline compounds. As examples of semicrystalline materials, isotactic polystyrene and polymethylmethacrylate were chosen. The proton spectra of these materials are shown in figures 10 and 11. The methoxy protons are clearly distinguishable from the methylene and methyl protons in polymethylmethacrylate. The ring and aliphatic protons are cleanly separated in polystyrene.

(ii) *Complex mixtures of solids: coals*

Perhaps one of the more complex materials previously inaccessible to analysis in its native state by any technique is coal. In the simple crystalline solids, or in simple polymers, one presumably need not spin the sample at speeds high compared with chemical shift anisotropies

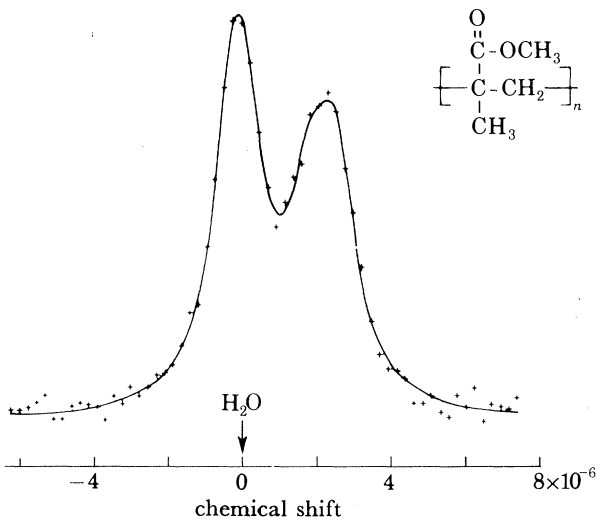

FIGURE 10. CRAMPS spectrum of ^1H in polymethylmethacrylate.

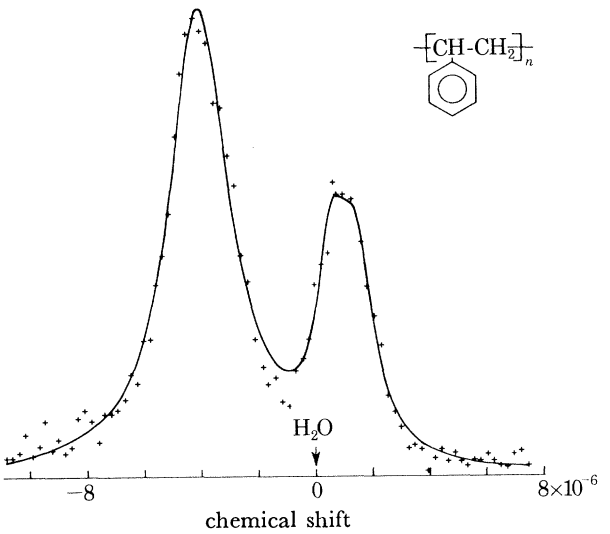

FIGURE 11. CRAMPS spectrum of ^1H in isotactic polystyrene.

to remove the shielding anisotropy contribution to the broadening (Maricq & Waugh 1979). The rotational echo technique, does not, however, work when inherently narrow lines are not present in the material under study. Coals have an enormous diversity of chemical structures, and as such have an almost continuous dispersion of isotropic proton chemical shifts covering both the aliphatic and aromatic regions of the spectrum. As an example of the type of analysis available from the proton n.m.r. of coals at a d.c. field of 1.327 T, the proton spectrum of a vitrain portion of an Iowa coal containing 75% C (moisture and ash free) is shown in figure 12. One can see two regions separated by about 5×10^{-6}, the aliphatic–aromatic proton separation. Proton aromaticities inferred from a diagnosis of spectra similar to these appear to increase with increasing carbon content, and are not in disagreement with proton aromaticities inferred from infrared spectroscopy (Ryan *et al.* 1981).

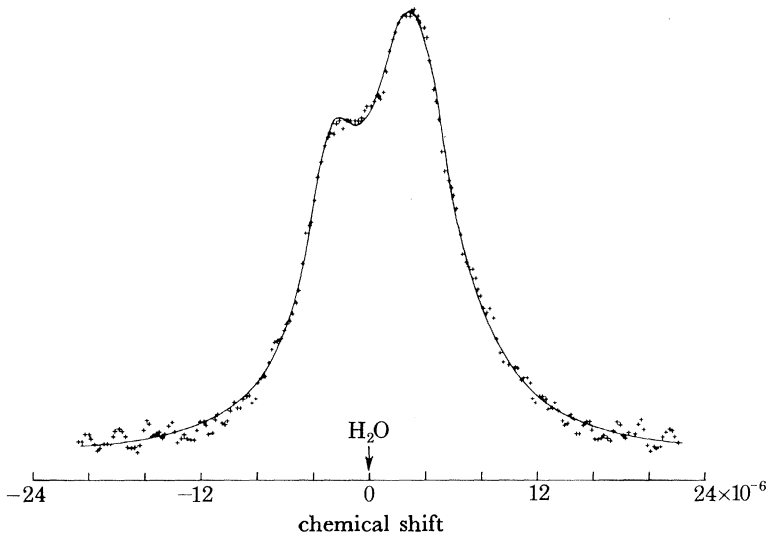

FIGURE 12. CRAMPS spectrum of protons in Lovilia vitrain coal.

TABLE 3. LINE-WIDTH RESULTS FOR MULTIPLE-PULSE AND CRAMPS MEASUREMENTS

(Full width at half height, results given in hertz.)

compound†	i.p.	PMMA	DMBP	DMBA
CRAMPS (8-pulse) aliphatic line	157	230	156	145
CRAMPS (8-pulse) aromatic line‡	160	110	170	131, 74§
CRAMPS (24-pulse) aliphatic lines	CH CH_2	CH_2 CH_3		
	69 74	79 65	109	88
CRAMPS (24-pulse) aromatic lines‡	141	77	62,‖	59,‖ 65,¶
			109¶	76§
MREV-8	586	431	552	466
P_x–M_y	11	15	4	3
$-M_x$	71	67	34	47

† PMMA, polymethylmethacrylate; i.p., isotactic polystyrene; DMBP, 4,4′-dimethylbenzophenone; DMBA, 2,6-dimethylbenzoic acid.
‡ OCH_3 for PMMA.
§ OH.
‖ High field aromatic line.
¶ Low field aromatic line.

(iii) *Contributions to the line width*

As discussed in §2*e*, it is possible to sort out some contributions to the line widths of spectra of strongly homonuclear broadened solids with various pulse experiments. In table 3 are indicated residual contributions to proton line widths under MREV-8 and BR-24 sequences for the compounds with spectra shown in figures 8–11. It is seen that lifetime broadening, the upper limit of which is inferred from the $P_x - M_y$ experiment, is of order of 0.1×10^{-6} for the crystalline compounds, and of order of 0.2×10^{-6} for the polymers. Broadening associated with susceptibility dispersion is probably the main contribution to the line widths under CRAMPS, and is roughly 1×10^{-6} for the crystalline materials, and larger for the polymers. It is felt that the main source of static field dispersion in the crystalline materials is that due to non-uniform demagnetization fields of irregularly shaped crystallites (Fung *et al.* 1980). This broadening, unfortunately, scales linearly with field.

The effect of increased offset and increasing cycle time upon resolution of proton spectra of the compounds discussed herein have been investigated, and are detailed elsewhere (Ryan *et al.* 1980). It suffices to say that there is a value of offset, generally in the neighbourhood of 1 kHz, at which maximum resolution is obtained. Decreased cycle time always leads to increased resolution for the compounds discussed in this work (but see Dybowski & Pembleton 1979). The details of the interaction between the offset and dipolar operators have been discussed at length by Burum & Rhim (1979).

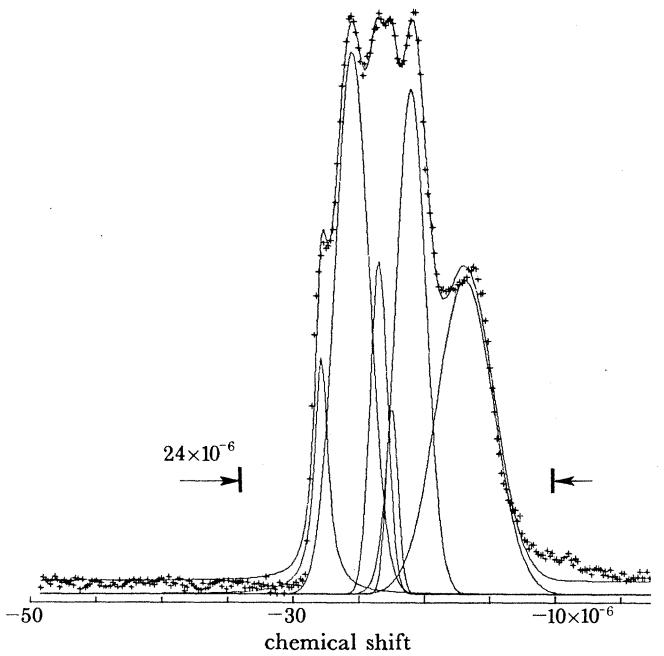

FIGURE 13. N.m.r. spectrum of ^{1}H in undiluted pentaoxyethylene dodecylether under magic angle spinning. Crosses, experimental points; curves, fit of peaks to a superposition of Lorentzian curves.

(iv) *Liquid crystals*

Chemical systems that appear to be begging for investigation by time-dependent techniques are those that are liquid-crystalline. So much of the behaviour of liquid crystals depends upon the details of motional phenomena in which there are enormous fluctuations. Rather than present a detailed account of applications of pulse n.m.r. to investigating liquid crystals, I should prefer to leave the reader with a *caveat*, and to illustrate the moral with an example. In figure 13 is shown the n.m.r. spectrum of ^{1}H in a liquid crystal made of a number of condensed ethylene glycol units, with an extended hydrocarbon chain attached to the end of the ethylene glycol polymer. This spectrum was taken under conditions of magic angle spinning. The spectral width is roughly 20×10^{-6} (much too large to be accounted for by the isotropic shielding values of the hydroxyl, methyne and methylene hydrogens in this compound). On the other hand, in figure 14 is shown the proton spectrum of the same compound taken under conditions of homonuclear decoupling only. The total spectral width in this case is only 5×10^{-6}. It is believed that molecular reorientation in the static field is sufficiently rapid for systems such as these, that magic angle spinning has not at all the same effect as it would have on a

rigid solid with dipolar broadening much smaller than the rotation rate. On the other hand, multiple-pulse decoupling does result in considerable narrowing, leaving, perhaps, shielding tensors severely modulated by molecular motion. The moral is clear. In the presence of motion, one must apply time-dependent techniques with eyes opened very wide indeed, which is an appropriate place to point to the future.

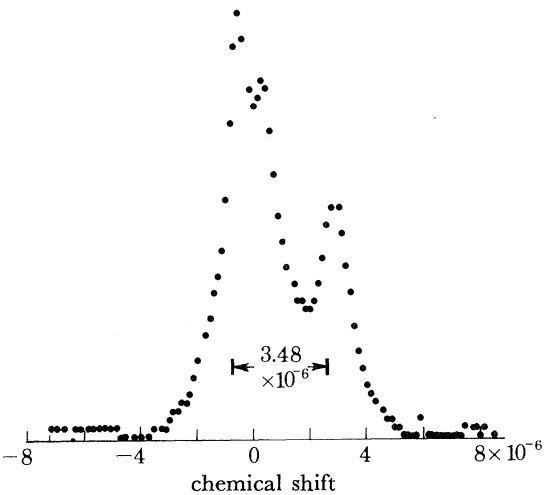

FIGURE 14. N.m.r. spectrum of protons in undiluted pentaoxyethylene dodecylether taken under conditions of homonuclear decoupling.

4. THE FUTURE

(*a*) *Relaxation under multiple-pulse decoupling*

The theory of relaxation under multiple-pulse experiments has been previously alluded to (Vega & Vaughan 1978). A most interesting area for application of this theory is that of materials undergoing relatively large librational motion, e.g. polymers and liquid crystals. Jasiński & Stachurowa (1979) have discussed effective decay times for systems undergoing rapid molecular reorientation, and it is an active area of research (Cheung *et al.* 1980). Just to mention one exciting possibility in this area, it appears that in at least two limiting cases, it is possible to perform a measurement of relaxation in the rotating frame ($T_{1\rho}$) in a one-shot experiment (Dybowski 1980).

(*b*) *Diffusion in rigid systems*

N.m.r. has been used to measure self-diffusion in liquids and in systems as viscous as glycerol; the range of diffusion constants measurable is from 10^{-5} to 10^{-8} cm^2 s. The standard technique for measuring slow diffusion has been by the pulse gradient experiment of Stejskal & Tanner (1965). This experiment depends upon the use of a refocusing 180° pulse to produce an echo, and works well when the only dephasing mechanism is associated with only an I_z operator, as discussed in the section on theory and average Hamiltonians. In relatively rigid systems, however, such as liquid crystals in the gel phase, dipolar broadening is a strong contributor to the transverse relaxation dephasing. Under this circumstance, it has been shown (Silva-Crawford *et al.* 1980) that the pulse gradient experiment, combined with multiple-pulse decoupling to remove dipolar interactions, can be used to monitor diffusion constants as low as

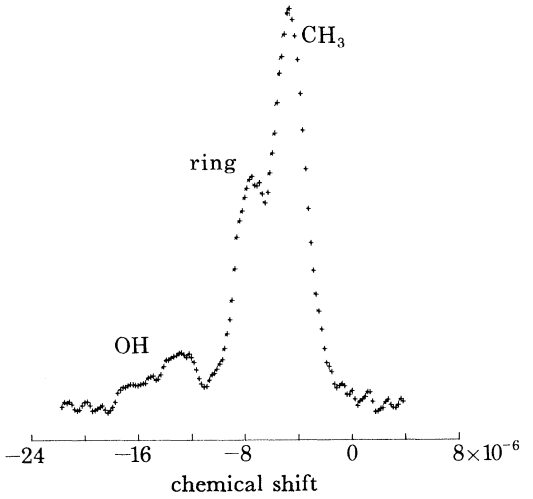

FIGURE 15. Recovery of proton tensors of off-magic angle spinning; n.m.r. spectrum of ^1H in 2,6-dimethylbenzoic acid. Compare the downfield region (the hydroxyl region) with the spectrum taken under homonuclear decoupling, but no spinning (figure 16) and with the CRAMPS spectrum of figure 9.

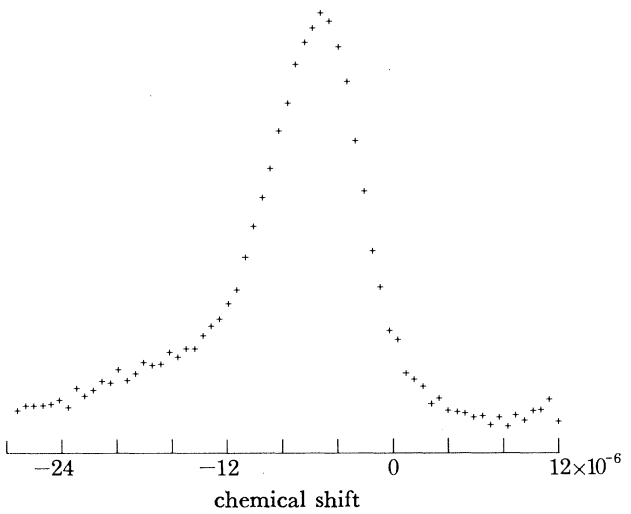

FIGURE 16. Spectrum of protons in 2,6-dimethylbenzoic acid under MREV-8.

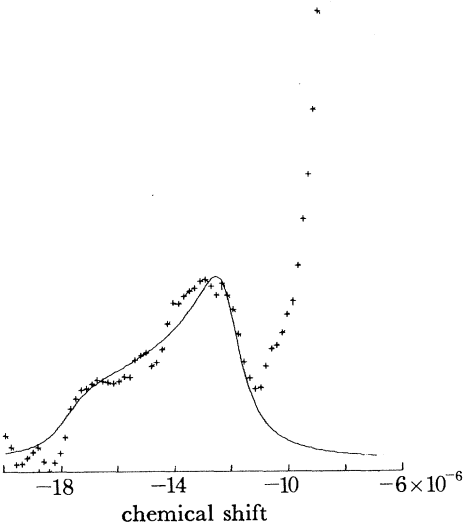

FIGURE 17. Expanded portion of the hydroxyl region in figure 15: fit of the hydroxyl tensor to an axially symmetric powder pattern scaled by $\frac{1}{2}(3\cos^2\theta - 1)$.

10^{-10} cm^2 s, and perhaps even an order of magnitude smaller. Applications to the study of lateral diffusion in membranes appear to be a very fruitful area of research.

(*c*) *Recovery of shielding anisotropies*

While the isotropic shift is an important piece of information, the full anisotropy of the shielding tensor is of course much more informative. A number of schemes have been suggested to recover the anisotropic information in experiments that yield both anisotropic and isotropic components where anisotropic tensors overlap badly (Maricq & Waugh 1979; Steiskal *et al.* 1977). My experience is with the use of off-magic angle spinning (o.m.a.s.). The basis for the

experiment is that under sample rotation at an angle θ to the applied field at sufficiently rapid rotation rates (Taylor *et al.* 1979) the shielding tensor becomes scaled by the factor $\frac{1}{2}(3\cos^2\theta - 1)$. Thus, a sample spun at an angle slightly larger or smaller than the magic angle will exhibit lines that bear the *symmetry* of the shielding tensors of the nuclei in the sample. However, the *magnitude* will be scaled, in some cases sufficiently to separate badly overlapping tensors, and the *sign* will depend upon the sign of the deviation from the magic angle. An example of the use of this technique to obtain the anisotropic components of the hydroxyl tensor in 2,6-dimethylbenzoic acid is shown in figures 15–17.

(*d*) *Dipolar oscillations, nuclear interferometry, etc.*

At some point one must decide when to bring a long list to a halt. The applications of homonuclear narrowing techniques mentioned, discussed or described in this paper are those that my prejudiced view hold to be promising. Others might choose quite a different list. In my opinion, however, two most recent developments that hold great promise, and which have not yet been alluded to, are (*a*) the use of dipolar oscillations to determine molecular structure (Müller *et al.* 1974; Hester *et al.* 1976; Stoll *et al.* 1976), and (*b*) the use of nuclear interferometry (Stoll *et al.* 1977; Polak *et al.* 1980, and references therein) to infer quadrupolar splitting of non-spin $\frac{1}{2}$ species.

The author's research is supported by the U.S. Department of Energy, contract no. W-7405-Eng-82, Division of Basic Energy Sciences, budget code AK-01-03-02-1. Thanks are due to coworkers T. T. P. Cheung, P. D. Murphy, L. M. Ryan, M. M. Silva-Crawford and R. E. Taylor.

References (Gerstein)

Adduci, D. J., Hornung, P. A. & Torgeson, D. R. 1976 *Rev. scient. Instrum.* **47**, 1503.
Adduci, D. & Gerstein, B. C. 1979 *Rev. scient. Instrum.* **50**, 1403–1415.
Anderson, P. W. 1954 *J. phys. Soc. Japan* **9**, 316–339.
Andrew, E. R., Bradbury, A. & Eades, R. G. 1958 *Nature, Lond.* **182**, 1659.
Andrew, E. R., Farnell, L. F., Firth, M., Gledhill, T. D. & Roberts, I. 1969 *J. magn. Reson.* **1**, 27–34.
Burum, D. & Rhim, W.-K. 1979 *J. chem. Phys.* **71**, 944–956.
Beams, J. W. 1930 *Rev. scient. Instrum.* **1**, 667–671.
Cheung, T. T. P., Gerstein, B. C., Ryan, L. M., Taylor, R. E. & Dybowski, C. R. 1980 *J. chem. Phys.* (In the press.)
Connor, T. M. 1970 *J. Polym. Sci.* A (2) **8**, 191–205.
Dybowski, C. R. 1980 Presented at the 21st Experimental Nuclear Magnetic Resonance Conference, Tallahassee, Florida, 19 March.
Dybowski, C. R. & Pembleton, R. G. 1979 *J. chem. Phys.* **70**, 1962–1966.
Dybowski, C. R. & Vaughan, R. W. 1975 *Macromolecules* **8**, 50–54.
Fung, B. M., Ryan, L. M. & Gerstein, B. C. 1980 *Biophys. J.* **29**, 229–236.
Gerstein, B. C., Chow, C., Pembleton, R. G. & Wilson, R. C. 1977 *J. phys. Chem.* **81**, 565–570.
Gerstein, B. C., Pembleton, R. G., Wilson, R. C. & Ryan, L. M. 1977 *J. chem. Phys.* **66**, 361–362.
Haeberlen, U., Ellett, J. D. & Waugh, J. S. 1971 *J. chem. Phys.* **55**, 53–62.
Haeberlen, U. & Waugh, J. S. 1968 *Phys. Rev.* **175**, 453–467.
Hester, R. K., Ackerman, J. L., Neff, B. C. & Waugh, J. S. 1976 *Phys. Rev. Lett.* **36**, 1081–1083.
Hwang, T. Y., Torgeson, D. R. & Barnes, R. G. 1978 *Phys. Rev. Lett.* A **66**, 137–140.
Jasiński, A. & Stachurowa, M. 1979 *Acta phys. polon.* A **55**, 433–439.
Krüger, G. J. 1969 *Z. Naturf.* **24**, 560–565.
Lau, K. F., Vaughan, R. W. & Satterthwaite, C. B. 1977 *Phys. Rev.* B **15**, 2449–2457.
Lowe, L. J. 1959 *Phys. Rev. Lett.* **2**, 285–287.
Mansfield, P. 1971 *J. Phys.* C **4**, 1444–1452.
Mansfield, P. & Haeberlen, U. 1973 *Z. Naturf.* **28a**, 1081–1089.
Mansfield, P., Orchard, M. J., Stalker, D. C. & Richards, K. H. B. 1973 *Phys. Rev.* B **7**, 90–105.

Maricq, M. M. & Waugh, J. S. 1979 *J. chem. Phys.* **70**, 3300–3316.
Müller, L., Kumar, A., Baumann, T. & Ernst, Richard R. 1974 *Phys. Rev. Lett.* **32**, 1402–1406.
Murphy, P. D. & Gerstein, B. C. 1978 *Designs of RF power amplifiers (high and low Q) and lumped equivalent circuits of transmission lines, with applications to NMR*, I.S 4596 (Available from Documents Library, Ames Laboratory U.S.D.O.E., Iowa State University, Ames, Iowa 50011, U.S.A.)
Murphy, P. D. & Gerstein, B. C. 1979 *J. chem. Phys.* **70**, 4552–4556.
Polak, M., Highe, A. J. & Vaughan, R. W. 1980 *J. magn. Reson.* **37**, 357–361.
Polak, M. & Vaughan, R. W. 1977 *Phys. Rev. Lett.* **39**, 1677–1680.
Resing, H. A. & Torrey, H. C. 1963 *Phys. Rev.* **131**, 1102–1104.
Rhim, W.-K., Burum, D. P. & Vaughan, R. W. 1976 *Rev. scient. Instrum.* **47**, 720–725.
Rhim, W.-K., Elleman, D. D., Schreiber, L. B. & Vaughan, R. W. 1974 *J. chem. Phys.* **60**, 4595–4604.
Rhim W.-K. Ellerman D. D. & Vaughan R. W. 1973 *J. chem. Phys.* **58**, 1772–1773.
Ryan, L. M., Murphy, P. D., Gerstein, B. C. & Solomon 1981 (In preparation.)
Ryan, L. M., Taylor, R. E., Paff, A. J. & Gerstein, B. C. 1980 *J. chem. Phys.* **72**, 508–515.
Ryan, L. M., Wilson, R. C. & Gerstein, B. C. 1977 *J. chem. Phys.* **67**, 4310–4311.
Silva-Crawford, M. M., Gerstein, B. C., Kuo, A.-L. & Wade, Charles G. 1980 *J. Am. chem. Soc.* (In the press.)
Slichter, C. P. & Ailion, D. 1964 *Phys. Rev.* A **135**, 1099–1110.
Stejskal, E. O. & Schaefer, J. 1975 *J. magn. Reson.* **18**, 560–563.
Stejskal, E. O., Schaefer, J. & McKay, R. A. 1977 *J. magn. Reson.* **25**, 569–573.
Stejskal, E. O. & Tanner, J. E. 1965 *J. chem. Phys.* **42**, 288–292.
Stoll, M. E., Vega, A. J. & Vaughan, R. W. 1976 *J. chem. Phys.* **65**, 4093–4098.
Stoll, M. E., Vega, A. J. & Vaughan, R. W. 1977 *Phys. Rev.* A **16**, 1521–1524.
Taylor, R. E., Pembleton, R. G., Ryan, L. M. & Gerstein, B. C. 1979 *J. chem. Phys.* **71**, 4541–4545.
Taylor, R. E., Silva-Crawford, M. M., & Gerstein, B. C. 1980 *J. Catal.* **62**, 401–403.
Torrey, H. C. 1954 *Phys. Rev.* **92**, 962–969.
Vega, A. J. 1980 Presented at the 21st Experimental Nuclear Magnetic Resonance Conference, Tallahassee, Florida, 19 March.
Vega, S., Shattuck, T. W. & Pines, A. 1976 *Phys. Rev. Lett.* **37**, 43–46.
Vega, A. J. & Vaughan, R. W. 1978 *J. chem. Phys.* **68**, 1958–1966.
Waugh, J. S., Huber, L. M. & Haeberlen, U. 1968 *Phys. Rev. Lett.* **20**, 180–182.
Wilcox, R. M. 1967 *J. math. Phys.* **8**, 962–982.
Zilm, K. W., Alderman, D. W. & Grant, D. M. 1978 *J. magn. Reson.* **30**, 563–570.

Discussion

K. J. Packer (*School of Chemical Sciences, University of East Anglia, Norwich, U.K.*). In multiple-pulse cycle sequences the main attention is directed to the question of averaging of homonuclear dipolar interactions and retention of chemical shielding effects. What are the effects of the various multiple pulse sequences on both homonuclear and heteronuclear indirect (scalar) couplings? Is it true that since the isotropic part of the scalar coupling is invariant to rotations, this is left unchanged (for homonuclear couplings), whereas since the heteronuclear coupling is similar in form to the chemical shielding (neglecting any flip-flop transitions between the non-resonant species), this interaction would be scaled in a similar manner to the chemical shift?

B. C. Gerstein. The scalar coupling is proportional to $I_z S_z$. If the species undergoing homonuclear decoupling is I, then the homonuclear decoupling experiment will only affect the I_z portion of the scalar interaction. This means that the scalar coupling will be scaled exactly as the chemical shift (which is also proportional to I_z) is scaled. In particular, under the MREV-8, both the chemical shift *and* the scalar coupling term will be scaled by $\frac{\sqrt{2}}{3}$ i.e. a scalar coupling that appeared to be 100 Hz under a single-pulse experiment will appear to be 47 Hz under the MREV-8.

K. J. Packer. Generally it is assumed that the effects of magic angle sample spinning (m.a.s.s.) and multiple-pulse averaging are independent so long as the cycle time of the latter is much

shorter than the rotor period. However, the effect of the multiple-pulse averaging leaves weaker, higher-order average Hamiltonian components that have an intrinsically longer time scale associated with them. Is it known whether these higher-order terms may themselves be further affected by m.a.s.s. whenever the rotor period is comparable with or shorter than the effective time scale associated with these already averaged, higher-order Hamiltonians? If so, in what way may they be affected?

B. C. GERSTEIN. My immediate response is that I probably do not know the answer to the question. A secondary response is that the two times in question are the cycle time of the multiple-pulse experiment (as a maximum when considering the action of the r.f. on the spin system) and the rotational cycle time of the m.a.s.s. (Note that the cycle time of the multiple-pulse experiment is an upper limit when asking about the time required for averaging of the homonuclear dipolar interaction. For example, the MREV-8 consists of two sequential WAHUHA-4 pulse cycles, both of which average the homonuclear dipolar interaction to zero to first order.) I therefore feel that if the r.f. cycle time is short (e.g. 0.1 t_{rot}) of the rotational cycle time, t_{rot}, then the static result obtains, and there is essentially no interaction between higher-order terms of the dipolar interaction, and the physical rotation experiment.

PHILOSOPHICAL TRANSACTIONS OF THE ROYAL SOCIETY A MATHEMATICAL, PHYSICAL & ENGINEERING SCIENCES

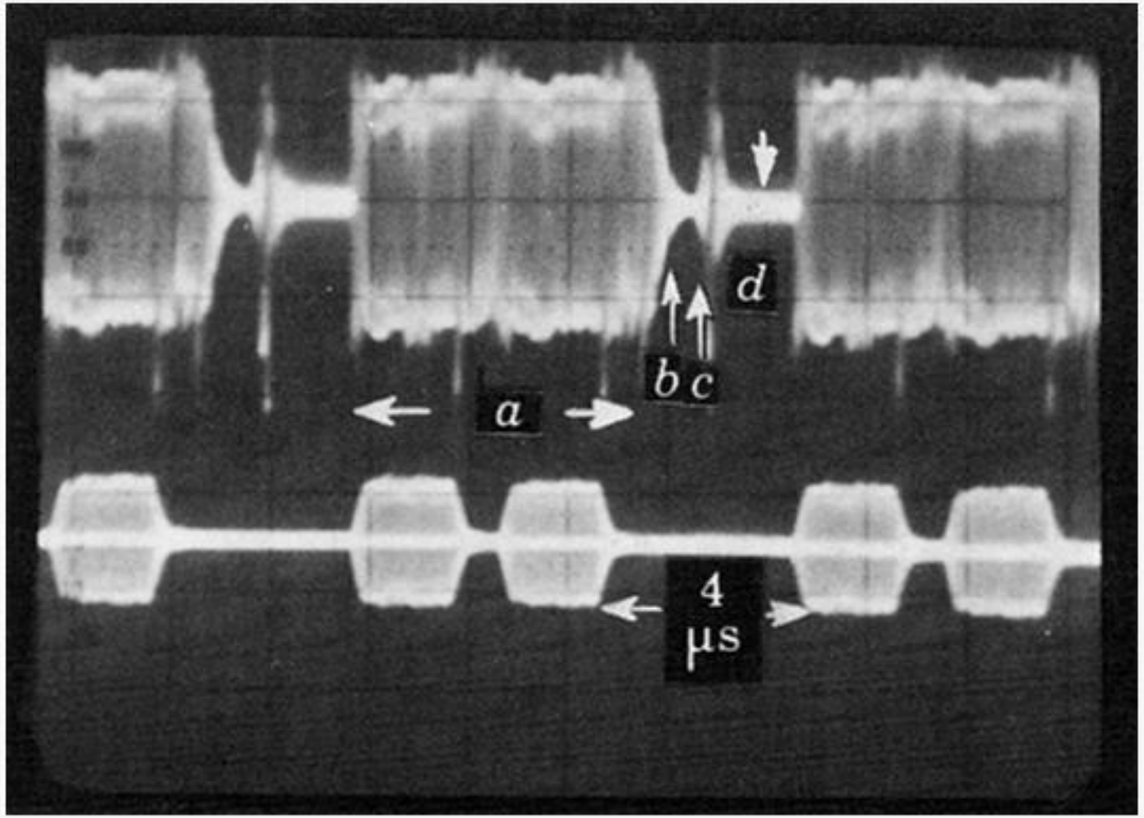

GURE 3. Comparison of signal detected at receiver output (top) and signal detected with antenna near probe (bottom). Receiver is one stage of an Avantek UTO 511 amplifier, followed by two stages of SML-D limiting amplifiers.